

REGULATION OF APE1 BY NEIL3 ZINC FINGER-GRF REPEAT ON SINGLE-
STRANDED DNA

by

Anh Ngoc Hoang Ha

A thesis submitted to the faculty of
The University of North Carolina at Charlotte
in partial fulfillment of the requirements
for the degree of Master of Science in
Biology

Charlotte

2020

Approved by:

Dr. Shan Yan

Dr. Christine Richardson

Dr. Junya Tomida

©2020
Anh Ngoc Hoang Ha
ALL RIGHTS RESERVED

ABSTRACT

ANH NGOC HOANG HA. Regulation of APE1 by NEIL3 Zinc Finger-GRF Repeat on Single-Stranded DNA. (Under the direction of DR. SHAN YAN)

Base excision repair (BER) is a critical pathway in repairing single base lesions caused by oxidation, deamination, and alkylation. NEIL3 is a DNA glycosylase which functions in initiating BER pathway by recognizing and removing damaged bases. Although there have been many studies reported on the function of NEIL3 in BER, the potential role of NEIL3 in the regulation of downstream BER players such as APE1 have not been dissected yet. In comparison to other Fpg/Nei glycosylase family members including NEIL1 and NEIL2, NEIL3 has two distinct zinc finger GRF motifs (Zf-GRF) in extreme C-terminus. In my thesis, two NEIL3 Zf-GRF motifs are my main focus due to their highly conserved residues across multiple vertebrates. Remarkably, my experimental observations reveal unexpected findings that two NEIL3 Zf-GRF motifs but not one Zf-GRF motif can interact and regulate APE1's endonuclease activity. In particular, I have demonstrated (1) two NEIL3 Zf-GRF motifs associate with APE1 but not APE2, (2) NEIL3 Zf-GRF motifs bind to single-stranded DNA (ssDNA) in a sequence-independent manner, (3) two Zf-GRF motifs allow for binding to shorter ssDNA compared with one Zf-GRF motif, and (4) the Zf-GRF repeat within NEIL3 compromises APE1's endonuclease activity on ssDNA. Taken together, my results suggest a distinct mechanism by which NEIL3 Zf-GRF repeat maintains genome stability of ssDNA via suppression of APE1 endonuclease activity-mediated DNA breaks.

ACKNOWLEDGEMENTS

I would like to thank Dr. Shan Yan, my advisor, for his support and advice on my research project from the start. As an advisor, he has been very helpful and guided me in term of which path should I take to complete my research project today. I also want to thank my committee members, Dr. Christine Richardson and Dr. Junya Tomida, for their willingness to meet and provide constructive criticisms for me to further improve my project. In addition, UNCC graduate school with financial assistance through Graduate Assistantships has been a great help for me to achieve my accomplishment today. I thank the National Institutes of Health for funding Yan lab. Finally, I would like to thank members of Yan lab for enormous knowledge they have taught me and their companionship.

TABLE OF CONTENTS

LIST OF FIGURES	vi
LIST OF ABBREVIATIONS	vii
CHAPTER 1: NEIL3-A UNIQUE DNA GLYCOSYLASE OF FPG/NEI FAMILY	1
1.1 Base excision repair (BER)	1
1.2 DNA glycosylases	2
1.3 Fpg/Nei Family: NEIL3	4
1.4 AP endonucleases	5
1.5 Zinc finger GRF motifs (Zf-GRFs)	7
1.6 Major hypothesis	9
1.7 Significance	10
CHAPTER 2: DETERMINATION OF THE ROLE OF NEIL3-ZF1&2 IN BER PATHWAY	12
2.1 Rationale and Hypothesis	12
2.2 Materials and Methods	13
2.3 Results	20
CHAPTER 3: DISCUSSION AND FUTURE DIRECTIONS	29
REFERENCES	42

LIST OF FIGURES

FIGURE 1: NEIL3 unique structure comparison among the Fpg/Nei family members	32
FIGURE 2: Coomassie protein expression verification for GST-NEIL3-ZF1 and GST-NEIL3-ZF1&2 and GST-NEIL3-ZF1&2 K553A	33
FIGURE 3: NEIL3-ZF1&2 interacts with APE1 and PCNA but not APE2 <i>in vitro</i>	34
FIGURE 4: NEIL3-ZF1&2 binds to shorter ssDNA than NEIL3-ZF1	35
FIGURE 5: NEIL3-ZF1&2 interacts with different ssDNA structures	36
FIGURE 6: MST assays show NEIL3-ZF1&2 motifs have higher binding affinity to Cy5-labelled 70-nt ssDNA than NEIL3-ZF1	38
FIGURE 7: NEIL3-ZF1&2 compromises APE1's endonuclease activity on ssDNA	39
FIGURE 8: NEIL3-ZF1&2 forms complexes with itself	40
FIGURE 9: A working model of the mechanism of NEIL3-ZF1&2 in the regulation of APE1's endonuclease activity on ssDNA	41

LIST OF ABBREVIATIONS

AP site: Apurinic/apyrimidinic site

APE1: Apurinic/apyrimidinic endonuclease 1

APE2: Apurinic/apyrimidinic endonuclease 2

BER: Base excision repair

cDNA: complementary DNA

Cy5: Indodicarbocyanine

dRP: deoxyribose phosphate

DSB: double-stranded break

dsDNA: double-stranded DNA

EEP: endonuclease/exonuclease/phosphatase

EMSA: Electrophoretic mobility shift assay

Fpg: Formamidopyrimidine DNA glycosylase

GST: Glutathione S-transferase

MST: Microscale thermophoresis

Nei: endonuclease VIII

NEIL1: Nei endonuclease VIII-like 1

NEIL2: Nei endonuclease VIII-like 2

NEIL3: Nei endonuclease VIII-like 3

nt: nucleotides

PAGE: Polyacrylamide gel electrophoresis

PCNA: proliferating cell nuclear antigen

PIP box: PCNA-interacting protein box

Pol β : DNA polymerase beta

Pol δ : DNA polymerase delta

Pol ϵ : DNA polymerase epsilon

SSBs: single-strand breaks

ssDNA: single-stranded DNA

THF: tetrahydrofuran

WT: wildtype

XRCC1: X-ray repair cross complementing 1

Zf-GRF/GRF-Zf: Zinc finger GRF

CHAPTER 1: NEIL3 – A UNIQUE DNA GLYCOSYLASE OF FPG/NEI FAMILY

1.1 Base Excision Repair (BER)

Genome of eukaryotic cells is under constant attack, both from exogenous agents such as ultraviolet (UV) radiation, chemotherapeutic drugs, ionizing radiation, etc. and from endogenous agents such as by-products generated from oxidative phosphorylation in mitochondria, resulting in vast majority of damages in DNA. These endogenous and exogenous agents introduce oxidative stress to these cells which is defined as an imbalance between the production of reactive metabolites termed reactive oxygen species (ROS) such as superoxide anion (O_2^-), hydrogen peroxide (H_2O_2), and hydroxyl radical ($\cdot OH$) and antioxidant defenses (Ray et al., 2012; Yan et al., 2014). DNA damage caused by oxidative stress has been implicated in aging and pathologies of human diseases, such as cancer and neurodegenerative disorders (Ray et al., 2012; Yan et al., 2014). Especially, when these damages accumulate, the chance for cell growth and reproduction interference is substantial. Thus, multiple DNA repair pathways have been evolved in the cells to deal with variety of damages ranging from single base lesions, mismatches, single-strand breaks (SSBs), to double-strand breaks (DSBs). Furthermore, a complex network called DNA damage response (DDR) is also triggered to coordinate the transcription activation and cell cycle progression with DNA repair (Ciccia & Elledge, 2010).

The basic and most common DNA repair pathway is base excision repair (BER) that deals with small base lesions produced by oxidation, deamination, and alkylation. Such lesions cause little to no distortion to DNA helix structure, but again, accumulation overtime certainly obstructs cellular processes. BER operates in five basic steps: (1)

recognition and excision of single base damage, (2) removal of apurinic/aprimidinic (AP) site, (3) end processing, (4) gap filling, and (5) ligation (Prakash & Doubleie, 2015). DNA glycosylases are required for initiation of BER by binding to minor groove, kinking DNA, and flipping the damaged base out of the major groove to generate AP (apurinic/aprimidinic) sites (Krokan & Bjoras, 2013). After the initiation by DNA glycosylase, AP sites are further cleaved to generate SSBs by APE1 or bifunctional DNA glycosylases (Krokan & Bjoras, 2013). BER proceeds as short-patch (or single nucleotide BER) which generates 1-nt gap or long-patch which results in 2-10nt replacement. Major core proteins for short-patch BER include X-ray repair cross-complementing protein 1 (XRCC1), Polymerase β (Pol β), and DNA ligase I or III (LIG1/3) that do not participate in replication (Krokan & Bjoras, 2013). Meanwhile, long-patch BER usually occurs in proliferating cells with a different set of core proteins such as Proliferating cell nuclear antigen (PCNA), Flap endonuclease 1 (FEN1), Polymerase δ/ϵ (Pol δ/ϵ), and DNA ligase I (LIG1) (Krokan & Bjoras, 2013). The choice of pathway, however, is heavily dependent on the type of initiating DNA glycosylase.

1.2 DNA glycosylases

So far, there have been more than 11 DNA glycosylases identified and classified into four superfamilies based on their conserved motifs and substrates that they recognize: Uracil DNA Glycosylase (UDG) family, the Alkyladenine DNA Glycosylase (AAG) family, Helix-Hairpin-Helix family (HhH), and the Formamidopyrimidine DNA Glycosylase (Fpg)/ Endonuclease VIII (Nei) (Prakash & Doubleie, 2015). UDG family members share common alpha-beta fold structured catalytic domain and excise uracil in both single-strand (ssDNA) and double-stranded DNA (dsDNA) (Jacobs & Schar, 2012). UDG

subfamily also works on pyrimidine derivatives in mismatches. Meanwhile, AAG family members recognize and remove a range of alkylated bases as well as methylated bases in ssDNA and dsDNA. These proteins lack helix-hairpin-helix motifs and alpha-beta fold (Jacobs & Schar, 2012). Both HhH and Fpg/Nei superfamilies have overlap substrates as they can both act on oxidative base damages. However, their conserved motifs are entirely different from each other as HhH family members have a shared helix-hairpin-helix domain while members of Fpg/Nei share a helix-two-turn-helix motif (Jacobs & Schar, 2012).

DNA glycosylases can be either monofunctional or bifunctional depending on their mechanistic steps following the recognition of damaged base for initiating BER. If DNA glycosylase is monofunctional, AP site is cleaved by APE1 to generate a 3'-hydroxyl (3'-OH) and 5'-deoxyribose phosphate (5'-dRP) (Krokan & Bjoras, 2013). 5'-dRP is then removed by Pol β to create 5' phosphate for ligation while inserting the correct nucleotide to the gap (Krokan & Bjoras, 2013). Bifunctional DNA glycosylase has either β -lyase activity or β,δ -lyase in addition to AP site generation function. With β -lyase, unsaturated hydroxyaldehyde linked to 3' end (3'-dRP) and 5' phosphate end is generated (Krokan & Bjoras, 2013). Then, 3'-OH is produced by the removal of 3'-dRP by APE1. With β,δ -lyase, however, 3'-phosphate and 5'-phosphate ends are generated for both sides of AP site. Then polynucleotide kinase/ 3'-phosphatase (PNKP) or APE1 trims the 3' phosphate into 3'-OH in order for BER to continue (Krokan & Bjoras, 2013). The specificity of 5' and 3' ends of AP site is critical for determining the downstream steps in BER.

DNA glycosylases are unique due to their ability to scan through the genome for damaged bases. With more than 10^4 base lesions per day, DNA glycosylases need to

develop strategies for efficiently searching for and recognizing base lesions (Jacobs & Schar, 2012). Although monofunctional and bifunctional glycosylases certainly employ different strategies, their overall principle of action is still quite similar. After DNA glycosylases recognize their substrates by rotating bases out into fitting pocket that contains active site, cleavage of N-glycosidic bond to result in free base and AP site will occur following successful base fitting. Different structure of each DNA glycosylase plays a critical role in the recognition and removal of damaged base. Thus, it is significant to study structure of Fpg/Nei protein NEIL3 to explain its mechanism in identification of single base lesions in the presence of vast excess regular bases.

1.3 Fpg/Nei Family: NEIL3

Fpg/Nei family had its name from bacterial prototypes Fpg and Nei that includes E.coli Nei and Fpg (EcoNei, EcoFpg) with the mammalian counterparts known as NEIL1, NEIL2, and NEIL3 (Krokan & Bjoras, 2013). Sequence alignments of all Fpg/Nei members reveal their hallmark structural similarities such as helix-two-turns-helix motif (H2TH) and a family zinc-finger motif (except NEIL1) with N-terminal proline (in NEIL1 and NEIL2) or valine residue (in NEIL3) as the active site nucleophile (Prakash et al., 2012). Overall, structure of these family members exhibits a classic 2-domain architecture where N and C-terminal domains connected by interdomain linker containing DNA binding groove (Prakash & Doublet, 2015). N-terminal domain consists of 2-layered β -sandwich capped in either end by α -helix (Prakash & Doublet, 2015). Thus, slight variations in structure among NEIL proteins contribute to different types of substrates that they can recognize as DNA glycosylases. NEIL1 works on lesions in dsDNA, bubble, bulge, and fork structures with the best substrates for NEIL1 including

oxidized pyrimidines such as Tg, 5-hydroxyluracil (5-OHU), dihydrouracil (DHU), etc. as well as ring opened Fapy lesions (Prakash & Doublie, 2015). In contrast, both NEIL2 and NEIL3 prefer lesions in ssDNA with substrates for NEIL2 similar to NEIL1 while NEIL3 works on FapyG, FapyA, spiroiminodihydroantoin (Sp), and guanidinohydroantoin (Gh) (Krokan & Bjoras, 2013).

NEIL3 structure demonstrates overall similarities in the N-terminal domain to *E.coli* Fpg/Nei and NEIL1, NEIL2 (Figure 1A). However, C-terminal domain of NEIL3 exhibits distinguished features that none of its family members has. The functions of RANbp-like zinc finger (RBP-Znf) and two GRF zinc-finger (Zf-GRF) motifs within NEIL3 remains unknown. Thus, in our study, we aimed to dissect the potential role of NEIL3 C-terminal Zf-GRF motifs in genome integrity and to determine why such Zf-GRF repeat appears in NEIL3 and absent from the rest of Zf-GRF-containing proteins.

1.4 AP endonucleases

Approximately 10,000 AP sites are generated in mammalian cells daily as cells are exposed to intensive oxidative stress (Dyrkheeva et al., 2016). Chemical reactivity of AP sites leads to formation of breaks in DNA molecule, so cells have AP endonucleases to combat such damages introduced inside the cells. AP endonucleases, specifically APE1, are the most critical enzyme in BER pathway which regulates the downstream steps in BER after the removal of AP sites occurs. APE1 has major contribution to AP site cleavage to generate SSBs with 3'-OH with 5'-dRP ends in DNA, and then, the DNA synthesis with ligation steps in BER are followed.

AP endonucleases are multifunctional proteins which are categorized into two families: exonuclease III (Exo III or Xth) or endonuclease IV (EndoIV or Nfo) depending on their

amino acid sequence similarity (Dyrkheeva et al., 2016). APE1 belongs to family related to ExoIII from *E.coli* which includes Rrp1 (*Drosophila melanogaster*), Apn2 (*Saccharomyces cerevisiae*), BAP1 (bovine), etc. The enzymes in this family have several activities including AP endonuclease, 3'-5' exonuclease, 3'-phosphodiesterase, and 3'-phosphatase on double-stranded DNA (dsDNA) (Dyrkheeva et al., 2016).

APE1 consists of a flexible N-terminal domain and C-terminal which is highly responsible for DNA interaction and AP endonuclease activity. APE1 comprises a four-layer α,β sandwich structure which is highly conserved characteristic for nucleases. The N-terminal domain (~60aa) is redox region for APE1 while the rest is DNA repair region (Dyrkheeva et al., 2016). APE1 is an abundant protein which can be found in nucleus, mitochondria, and in cytoplasm. APE1 inactivation is lethal for embryonic development in mice (Xanthoudakis et al., 1996). About 95% of total AP site cleavage is performed by APE1 in humans (Dyrkheeva et al., 2016). Initially, APE1 binds to DNA randomly and slides along the strand to search for AP site. The interaction between APE1 and DNA is through two enzyme sites: one with Met270 and Met271 residues for minor groove binding and one with Arg177 for major groove interaction which slows the dissociation of APE1 from product of endonuclease reaction (Dyrkheeva et al., 2016). Slow dissociation between APE1 and DNA prevents accumulation of SSBs. Notably, APE1 also functions on ssDNA although the activity is much lower compared to dsDNA (about 20-fold) and does not depend on the presence of DNA glycosylases (Dyrkheeva et al., 2016). Thus, APE1 activity toward ssDNA suggests potential functions in replication and transcription in cells.

Another type of AP endonucleases in the same ExoIII family is AP endonuclease 2 (APE2) which has significantly lower endonuclease activity than APE1 but robust PCNA-stimulated 3'-5' exonuclease and 3'-phosphodiesterase activities (Burkovic et al., 2009; Wallace et al., 2017). It has been shown that APE2 is necessary for normal B-cell development and recovery from chemotherapeutic drug induced DNA damage. Notably, APE2 participates in PCNA-dependent repair of H₂O₂-induced oxidative damage and is important for the activation of ATR-Chk1 DDR pathway following oxidative stress (Wallace et al., 2017; Willis et al., 2013). Structure of APE2 is unique as it carries additional Zf-GRF and PCNA-interacting protein box (PIP box) besides its catalytic endonuclease/exonuclease/phosphatase domain (EEP) (Figure 1A). APE2 interacts with PCNA which is also a critical protein in BER pathway long-patch to promote 3'-5' SSB end resection for activation of ATR-Chk1 DDR (Wallace et al., 2017). Interestingly, both APE1 and APE2 have been shown to be upregulated in cancer cell lines which is remarkably similar to the pattern observed in NEIL3 (Jensen et al., 2020; Manoel-Caetano et al., 2019; Qing et al., 2015; Shinmura et al., 2016). In addition, other proteins such as XRCC1, PCNA, and PARP1 have upregulated expression together with APE2 in tumors which suggests the APE2 participation in BER and DDR (Jensen et al., 2020).

1.5 Zinc finger GRF motifs (Zf-GRFs)

Zinc finger proteins (ZFs) are most abundant groups of proteins with various types of zinc finger domains. ZF proteins have key role in development and differentiation of tissues as well as involving in tumorigenesis and cancer progression. ZF can interact with DNA, RNA, PAR (poly-ADP-ribose) and proteins (Cassandri et al., 2017). ZFs are

important for regulation of several cellular processes including transcriptional regulation, signal transduction, actin targeting, DNA repair, cell migration, etc. The simple and basic ZF structure was identified in 1980s in Transcription Factor III_s (TFIII_s) from *Xenopus laevis* with zinc ion in the center surrounded by 2 cysteine (C2) in one chain and 2 histidine (H2) in another chain which form C2H2 ZF type (Cassandri et al., 2017). Currently, 30 types of ZFs have been identified, and among them, the least studied ZF type is Zf-GRF.

Zf-GRF motif has three conserved residues found in such structure: Glycine (G), arginine (R), and phenylalanine (F). TIF2 (nuclear receptor coactivator 2), NEIL3, APE2, and TOP3A (DNA Topoisomerase III Alpha) are some represented proteins containing Zf-GRF domain(s) (Cassandri et al., 2017; Wallace et al., 2017). APE2 Zf-GRF motif is one of the first Zf-GRF that has been characterized so far (Figure 1A) (Wallace et al., 2017). Structural analysis reveals that Zf-GRF in APE2 consists of three β -sheets harboring Zn²⁺ and GRF which folds into crescent-shaped claw-like structure specific for ssDNA and is required for 3'-5' end resection on damaged DNA (Wallace et al., 2017).

Consistent with the preferential binding of APE2 Zf-GRF to ssDNA but not dsDNA (Wallace et al., 2017), it is also reported that *Xenopus* NEIL3 associates with ssDNA in vitro (Wu et al., 2019). With such knowledge, in our study, we aim to characterize NEIL3 Zf-GRF motifs as not only we want to see if conserved motifs can result in similar functions as shown in APE2 Zf-GRF regardless of protein types but also if having two Zf-GRF motifs is required for NEIL3 function in BER rather than one or none Zf-GRF motifs.

1.6 Major Hypothesis

NEIL3 N-terminal domain has been characterized as well-known catalytic domain that is responsible for DNA glycosylase in BER to maintain genome stability. However, there is little information about C-terminal domain, specifically the two Zf-GRF motifs. A recent study has demonstrated that NEIL3 plays a crucial role in telomere repair and that depleting NEIL3 causes telomere dysfunction and mitotic defects (Zhou et al., 2017). A critical finding from this study is about how NEIL3 can interact to core proteins in long-patch BER, particularly PCNA and FEN1 but not short-patch BER protein Pol β .

Furthermore, APE1 shows strong interaction to NEIL3 in cell lysates (Zhou et al., 2017).

Additional analysis reveals that C-terminal domain but not N-terminal domain of NEIL3 is responsible for such interaction to APE1 (Zhou et al., 2017). This result indicates that NEIL3 requires its C-terminal domain to maximize NEIL3 activity as DNA glycosylase.

For DNA binding ability, NEIL3 demonstrates strong interaction to ssDNA, G-quadruplex DNA, and dsDNA although the interaction to dsDNA is very weak (Zhou et al., 2017). In addition, when testing with biotinylated ssDNA mimicking G-strand and C-strand telomere sequences (ssG or ssC in order) and dsDNA, NEIL3 full length and C-terminal domain NEIL3 can pulldown these DNA structures (Zhou et al., 2017).

Especially, C-terminal domain shows very strong interaction to ssG and ssC while N-terminal shows very weak to no interaction at all to these structures. Yet, specific motifs responsible for protein-protein interaction and DNA binding ability in NEIL3 have not been identified and characterized in more details.

Our research focuses on two NEIL3 Zf-GRF motifs to study their function and possibly explain why NEIL3 needs extra motifs in C-terminus, especially when they make NEIL3

longer and bulky compared to the rest of its family members. The objective of our research is to determine the role of NEIL3 Zf-GRF motifs in genome integrity. Our major hypothesis is that two Zf-GRF motifs in NEIL3 are required for its distinct role in DNA interaction and regulation of other repair protein(s) in genome integrity. We have two specific aims to test our hypothesis:

Aim 1: Determine how NEIL3-ZF1&2 interacts with different DNA structures

Aim 2: Determine how NEIL3-ZF1&2 interacts with PCNA and APE1 in BER

1.7 Significance

The findings will explain why NEIL3 in this Fpg/Nei family is the only protein carries two Zf-GRF motifs and examine the consequences of removing one out of two Zf-GRF motifs. Two questions can be answered in this study as why NEIL3 needs two Zf-GRF motifs and what are the functions of such motifs in BER pathway. In addition, this study is unique as one of the first studies performed on two Zf-GRF motifs which later on can be used as starting guide for other researches on Zf-GRF motifs, especially on proteins that have more than one Zf-GRF. In general, Zf-GRF motifs have not been characterized intensely as so far, only APE2 Zf-GRF motif has been studied recently. Unfortunately, only minimal information of APE2 Zf-GRF motif can be used for this research as not only APE2 has just one Zf-GRF motif but also APE2 and NEIL3 are two completely different proteins. APE2 is AP endonuclease while NEIL3 is DNA glycosylase, so even though structural comparison reveals some similarities, when putting into big picture, APE2 Zf-GRF motif will be likely different from NEIL3 Zf-GRF motifs.

Another interesting aspect about NEIL3 is its over expression during S/G2 phase which indicates its possible role in DNA replication and cell proliferation (Zhou et al., 2017).

Furthermore, reduced expression of NEIL1 and NEIL2 with elevated expression of NEIL3 are found in 13 cancer types, suggesting that abnormal expression of NEIL1, NEIL2, and NEIL3 are associated with cancer etiology (Shinmura et al., 2016). By understanding the structure and function of NEIL3, especially C-terminal domain, its function will be revealed further and its over expression in certain stage of cell division as well as in tumor can be partially explained.

CHAPTER 2: DETERMINATION OF THE ROLE OF NEIL3-ZF1&2 IN BER PATHWAY

2.1 Rationale and Hypothesis

Prior study has shown that NEIL3 C-terminal domain associates with ssDNA (Zhou et al., 2017). Thus, we sought to test if two NEIL3 Zf-GRF motifs by themselves will demonstrate such characteristic. At the same time, we want to reveal the length limitation of ssDNA that NEIL3 Zf-GRF motifs can bind to. In addition, we would like to find out why two Zf-GRF motifs within NEIL3 are necessary for its function in genome integrity. By depleting one out of the two Zf-GRF motifs and by mutating one of two Zf-GRF motifs can help us to understand the importance of two Zf-GRF motifs in NEIL3.

It has been shown in a previous study that NEIL3 interacts with long-patch BER core proteins such as PCNA and FEN 1, and that NEIL3 C-terminal domain is responsible for the interaction between NEIL3 and APE1 (Zhou et al., 2017). We recently demonstrate that APE1 but not XRCC1 senses DNA SSBs for repair and signaling in *Xenopus* egg extracts (Yan et al., 2013; Cupello et al., 2016&2019; Lin et al., 2019&2020). Thus, we sought to express and purify recombinant two NEIL3 Zf-GRF motifs and determine whether NEIL3 Zf-GRF motifs associate with the BER proteins directly via *in vitro* protein-protein interaction assays. If there is interaction detected, we would like to dissect the domain requirements of the interaction between NEIL3 Zf-GRF motifs and BER proteins.

In this chapter we will test two hypotheses: First hypothesis is that two NEIL3 Zf-GRF motifs are required for binding to short ssDNA. Second hypothesis is that two NEIL3 Zf-GRF motifs can interact with APE1 and regulate its function in genome integrity.

2.2 Materials and methods

Preparation of GST-NEIL3-ZF1&2, GST-NEIL3-ZF1, and GST-NEIL3-ZF1&2

K553A recombinant proteins

Recombinant plasmid pGEX4T1-NEIL3-ZF1&2 was prepared by PCR coding sequence for two NEIL3 ZF-GRF from *Xenopus laevis* NEIL3 cDNA (GenBank: BC072255.1) with a pair of primers (Forward primer #1: 5'-CCCCCGGATCCCCACAGTGCAGTGCACACAATGTTC-3' and Reverse Primer #1: 5'-CCCCCCTCGAGCTACTCTGTTTTTGCCCATTC-3') and inserting into pGEX4T1 vector at BamHI and XhoI sites. Then, DH5 alpha cells were used to amplify the recombinant plasmid. Recombinant pGEX4T1-NEIL3-ZF1&2 plasmid was verified using sequencing for correct insertion. Plasmid pGEX4T1-NEIL3-ZF1&2 was then expressed in DE3 cells with IPTG induction, and the recombinant GST-NEIL3-ZF1&2 protein was purified following vendor's procedure. Successful isolation of GST-NEIL3-ZF1&2 was checked by Coomassie with GST as control. Similar procedure was used to express and purify GST-NEIL3-ZF1 with exception that the PCR process for pGEX4T1-NEIL3-ZF1 required a different pair of primers (Forward primer #1 and Reverse Primer #2: 5'-CCCCCCTCGAGCTAGTCTGCCATTCAAATATTGACAAC-3').

To generate pGEX4T1-NEIL3-ZF1&2 K553A, two single-primer PCR reactions were set up using forward primer #2: 5'-GAAGATTGGCCCAAACAACGGAGCGAATTTTTACGTCTGCCCGATGG-3' and reverse primer #3: 5'-CCATCGGGCAGACGTAAAAATTCGCTCCGTTGTTTGGGCAATCTTC-3' with methylated parental plasmid pGEX4T1-NEIL3-ZF1&2. After PCR, two reactions were

combined and denatured at 95°C and cooled for random annealing. DpnI was added for digesting methylated, non-mutated parental DNA strands at 37°C overnight. Then, DH5 alpha cells were used to amplify the plasmid. Sequencing was used to verify if the plasmid contained the correct mutation before protein expression and purification steps. Plasmid pGEX4T1-NEIL3-ZF1&2 K553A was then expressed by DE3 cells with IPTG induction similar to the procedure indicated above for GST-NEIL3-ZF1&2. Successful expression of GST-NEIL3-ZF1&2 K553A was verified by Coomassie using GST as control.

Preparation of Myc-NEIL3-ZF1&2, Myc-NEIL3-ZF1, and Myc-NEIL3-ZF2

To generate Myc-NEIL3-ZF1&2, pGEX4T1-NEIL3-ZF1&2 plasmid was used in PCR with designed forward primer and previously described reverse primer (Forward Primer #3: 5'-CCCCCGAATTCACCACAGTGCAGTGCACACAATGTTC-3' and Reverse Primer #1). pCS2+MT as vector together with amplified PCR sequence were digested with EcoRI and XhoI (NEB) at 37°C for two hours and were ligated. pCS2+MT-NEIL3-ZF1&2 was obtained, and 1µL of recombinant plasmid was added into 10µL TNT SP6 at 30°C for 90 minutes for Myc-NEIL3-ZF1&2 protein expression.

Similar procedure was utilized to generate Myc-NEIL3-ZF2 by using two primers (Forward Primer #4: 5'-CCCCCGAATTCACCATTCTGCAACCATGGGAAAC-3' and same Reverse Primer #1). For Myc-NEIL3-ZF1, two primers were utilized similarly (Forward Primer #3 and Reverse Primer #2).

Preparation of GST-APE1, Myc-APE1, Myc-APE1 E95Q, Myc-APE1 E95Q-D209N, Myc-APE1 D306A, and Myc-APE2

Xenopus laevis recombinant plasmids pGEX4T1-APE1, pCS2+MT-APE1, pCS2+MT-APE1 D306A, and pCS2+MT-APE2 were described previously (Lin et al., 2018; Lin et al., 2020; Willis et al., 2013). Recombinant plasmid pCS2+MT-APE1 E95Q was generated based on pCS2+MT-APE1 template using designed primers (Forward primer #5: 5'-GACCCACACATCATGTGTCTCCAGCAAATAAAAATGTGCAGAGAAATTG-3' and Reverse primer #5: 5'-CAATTTCTCTGCACATTTTATTTGCTGGAGACACATGATGTGTGGGTC -3') with site-directed mutagenesis kit. Once the plasmid was made, mutant plasmid was validated via sequencing. Similarly, the same procedure was utilized for pCS2+MT-APE1 E95Q-D209N with pCS2+MT-APE1 E95Q as template and Forward primer #6: 5'-GAAGCCATTAATACTGTGTGGTAATCTGAATGTGGCGCACCAGG -3' and Reverse primer #6: 5'-CCTGGTGCGCCACATTCAGATTACCACACAGTATTAATGGCTTC -3'.

Recombinant Myc-tagged proteins were expressed in the TNT SP6 Quick Coupled Transcription/translation system at 30°C for 90 minutes using respective recombinant plasmid subcloned in pCS2+MT vector.

Preparation of 5'-Biotin and 5'-FAM labeled ssDNA and dsDNA structures

Different sizes of Biotin-ssDNA: 10, 20, 40, and 60 nucleotides (nt) were generated with biotin labeled to 5' side by vendor with sequences indicated below.

- Biotin-10nt: [Biotin~5]GGTCGACTCT
- Biotin- 20nt: [Biotin~5]GGTCGACTCTAGAGGATCCC

- Biotin- 40nt:

[Biotin~5]GGTCGACTCTAGAGGATCCCCGGGTACCGAGCTCGAATTC

- Biotin- 60nt:

[Biotin~5]GGTCGACTCTAGAGGATCCCCGGGTACCGAGCTCGAATTCAC
TGGCCGTCGTTTTACAAC

5'-FAM labeled 39nt-dsDNA that contains AP site-mimicking tetrahydrofuran (THF) (designed as dsDNA39-AP) was generated by annealing forward and reverse primers (Forward Primer #7: 5' FAM-

TGCTCGTCAAGAGTTCGTAA(THF)ATGCCTACACTGGAGATC -3' and Reverse Primer #7: 5' - GATCTCCAGTGTAGGCATCTTACGAACTCTTGACGAGCA -3').

The mixture was incubated at 95-100°C for 5 minutes with mixing every minute during incubation. The mixture was slowly cooled down naturally at room temperature for 30-45 minutes. 5'-FAM labeled ssDNA with THF (designed as ssDNA39-AP) was generated using only the forward primer indicated above (Forward Primer #7) with no further step needed. 5'-FAM labeled 39nt-ssDNA without THF site (designed as ssDNA39) was synthesized by vendor (Forward Primer #8: 5' FAM-

TGCTCGTCAAGAGTTCGTAACATGCCTACACTGGAGATC -3').

5'-FAM labeled 70nt-ssDNA (designed as ssDNA70) was generated with designed forward primer (Forward Primer #9: FAM-5'-

TCGGTACCCGGGGATCCTCTAGAGTCGACCTGCAGGCATGCAAGCTTGGCGT AATCATGGTCATAGCTGT -3'). 5'-Cy5-labeled 70nt-ssDNA (designed as Cy5-

ssDNA70) (Forward Primer #10: Cy5-5'-

TCGGTACCCGGGGATCCTCTAGAGTCGACCTGCAGGCATGCAAGCTTGGCGT

AATCATGGTCATAGCTGT -3') was synthesized by vendor, which was used only for MST binding affinity experiments. In addition, 5'-FAM labeled 70nt-ssDNA with 3'-Biotin end was produced based on the similar sequence as 70nt 5'-FAM labeled ssDNA above but with biotin attached to 3' (designed as ssDNA70-BIOTIN) (Forward Primer #11: FAM-5'-

TCGGTACCCGGGGATCCTCTAGAGTCGACCTGCAGGCATGCAAGCTTGGCGT
AATCATGGTCATAGCTGT -3'-Biotin).

Biotin-DNA binding assays

Different biotin-labeled DNA structures were coupled to Streptavidin Dynabeads using the approach previously described (Lin et al., 2018). The beads were mixed with GST or GST-tagged recombinant proteins including GST-NEIL3-ZF1&2 and GST-NEIL3-ZF1 at room temperature for 60 minutes. The beads were washed by Buffer A (80mM NaCl, 20mM β -Glycerophosphate, 2.5mM EGTA, 0.01% NP-40, and 10mM HEPES-KOH, pH7.5). The input and bead-bound fractions were examined via immunoblotting analysis using anti-GST antibodies.

GST-pulldown assays

Glutathione beads was incubated with 5 μ g of GST or GST-tagged recombinant proteins for an-hour binding at room temperature. Then, wild type his-PCNA (WT-PCNA) or 10 μ L of TNT SP6 reactions containing various Myc-tagged recombinant proteins was added to 500 μ L of Buffer B (100 mM NaCl, 5 mM MgCl₂, 10% (vol/vol) glycerol, 0.01% Nonidet P-40, 20 mM Tris-HCl at pH 8.0). The samples were incubated overnight at 4°C with rotation. After incubation, the samples were washed by Buffer C (100 mM NaCl, 5 mM MgCl₂, 10% (vol/vol) glycerol, 0.1% Nonidet P-40, 20 mM Tris-HCl at pH

8.0) twice to remove nonspecific binding proteins. The input and bead-bound fractions were examined via immunoblotting analysis.

Electrophoretic mobility shift assays (EMSA)

Different doses of GST-NEIL3 ZF1&2/ GST-NEIL3-ZF1/ GST-NEIL3-ZF1&2 K553A were incubated with 500nM of different 5'-FAM labeled ssDNA structures in Buffer D (10mM Tris, pH 8.0, 50mM NaCl, 0.2mM TCEP, and 5% glycerol) at room temperature for 60 minutes with mixing every 20 minutes. Then, 5x Hi-Density TBE Sample Buffer was added to each sample before running. Samples were resolved on 5% TBE gel at 150V for 2-3 hours in cold 0.5X TBE running buffer. Then, the gel was visualized using BIO-RAD Chemidoc MP Imaging System.

Microscale thermophoresis (MST) assays

50nM of Cy5-70nt-ssDNA was used as substrate and was checked via Pretest function in MST Monolith NT.115 to determine fluorescence intensity, adsorption on capillaries, variations and sample aggregation. Once verified, Binding Affinity option in MST instrument was selected with maximum dose of NEIL3-ZF1&2 used as base line for other proteins: GST, GST-NEIL3-ZF1, and GST-NEIL3-ZF1&2 K553A. 36µM of NEIL3-ZF1&2 was used for each trial, for a total of four trials. Series dilutions were generated following direction indicated in MST instrument. Buffer A was used for both substrate and ligand dilutions. 25°C was set as temperature control for all MST experiments performed. 16 Monolith NT.115 Capillaries were utilized for each trial per ligand. Besides NEIL3-ZF1&2, other ligands had three trials each. The results obtained were analyzed via MO Affinity Analysis v2.3 software as combination of trials for all ligands tested.

In vitro endonuclease assays

The 5'-FAM dsDNA-AP or ssDNA-AP structure was treated with different concentrations of purified GST-NEIL3-ZF1&2 or GST-NEIL3-ZF1 and 0.75 μ M GST-APE1 in Buffer E (20mM KCl, 10 mM MgCl₂, 2 mM DTT, 50 mM HEPES, pH 7.5) with GST only as control at 37°C for 60 minutes. Then, the reactions were quenched with equal volume of 2xTBE-Urea Sample Buffer, denatured at 95°C for 5 minutes. After a quick 10-second spin, samples were resolved on a 18% TBE-Urea gel in 1x TBE running buffer at 20,000W for 2 hours. Gels were viewed using BIO-RAD Chemidoc MP Imaging System.

For shielding effect experiment (Figure 7C), 5'-FAM-ssDNA39-AP was incubated with or without 10 μ M of GST-NEIL3-ZF1&2 for 3 minutes at 37°C. Different concentrations of purified GST-APE1 were added together with Buffer E into each sample. All samples were incubated at 37°C for 60 minutes before adding 2xTBE-Urea Sample Buffer. For inhibition effect experiment (Figure 7D), different concentrations of GST-APE1 was incubated with or without 10 μ M of GST-NEIL3-ZF1&2 for 3 minutes at 37°C. Then, 5'-FAM-ssDNA39-AP was added into each sample together with Buffer E. All samples were incubated at 37°C for 60 minutes prior to the addition of 2xTBE-Urea Sample Buffer. Later steps were repeated similarly as indicated above.

Different dilutions of GST-APE1 were incubated with or without 10 μ M of GST-NEIL3-ZF1&2 together with 5'-FAM labeled dsDNA39-AP structure in Buffer E (Figure 7E and 7F). All samples were incubated at 37°C for 60 minutes. Thus, the above procedure was repeated for dose dependent APE1 experiment.

2.3 Results

NEIL3 contains distinct Zf-GRF motifs in its extreme C-terminus

Compared with NEIL1 and NEIL2, the least-characterized NEIL3 displays a RBP-Znf motif and two Zf-GRF motifs (designated as ZF1 and ZF2) in its C-terminal domain (Figure 1A). Sequence alignment of ZF1 and ZF2 across four different species (*Xenopus laevis* (*Xl*), *Xenopus tropicalis* (*Xt*), *Mus musculus* (*Ms*), and *Homo Sapiens* (*Hs*)) showed highly conserved residues in each ZF motif (Figure 1B). Similar to APE2 Zf-GRF motif (Wallace et al., 2017), NEIL3 ZF1 contains the three conserved core amino acids: glycine (G), arginine (R), and phenylalanine (F); however, lysine (K) replaces arginine (R) to produce a Zf-GKF motif in NEIL3 ZF2 (Figure 1B). Although lysine and arginine have positive charge, their structures are much different with ionic interactions formed by arginine has shown to be more stable than lysine (Sokalingam et al., 2012). In addition, this replacement has been found across all four species indicates possible unique function that ZF2 might add into NEIL3 Zf-GRF motifs overall.

Furthermore, both ZF1 and ZF2 within NEIL3 contain the conserved CHCC-type Zn²⁺ contact motif (Figure 1B). Prior to the APE2 Zf-GRF motif, there is an alpha 1-helix and a proline-rich helix; however, it seems that no such motifs were found in the two Zf-GRF motifs in NEIL3 (Figure 1C).

Another unique aspect of the NEIL3 Zf-GRF motifs is the repeat of Zf-GRF in NEIL3 while APE2 contains only one Zf-GRF (Figure 1A). Sequence alignment revealed the distinctiveness of NEIL3-ZF-GRF-2 as the only one had lysine (K) while APE2 had arginine (R) in Zf-GRF motif (Figure 1C).

NEIL3-ZF1&2 interacts with APE1 and PCNA but not APE2

A recent study using co-immunoprecipitation assays from cell lysates expressing NEIL3-HA revealed the interactions of NEIL3 to BER proteins FEN1, APE1, and PCNA (Zhou et al., 2017). Further analysis showed that N-terminal domain of NEIL3 was not sufficient for the interaction to APE1 while full length NEIL3 could (Zhou et al., 2017). Although the C-terminal of NEIL3 seemed to be the key for such interaction between NEIL3 and APE1, it has not been identified which part in the C-terminal domain of NEIL3 is required or sufficient for APE1 interaction. Thus, we hypothesized that NEIL3-GRF-ZF1&2 is sufficient for APE1 interaction. To test this, we first expressed and purified GST-NEIL3-ZF1&2, GST-NEIL3-ZF1, and GST-NEIL3-ZF1&2-K553A (Figure 2A,2B).

Indeed, we found that GST-NEIL3-ZF1&2, but not GST nor GST-NEIL3-ZF1, interacted with Myc-APE1 (Figure 3A). Furthermore, our reciprocal experiment showed that GST-APE1, but not GST, associated with Myc-NEIL3-ZF1&2 (Figure 3D). Notably, neither Myc-NEIL3-ZF1 nor Myc-NEIL3-ZF2 was found to interact with GST-APE1 (Figure 3D). These observations suggest that two NEIL3 Zf-GRF motifs are required and sufficient for APE1 interaction and that one Zf-GRF within NEIL3 is defective for APE1 association (Figure 3A, 3D). To dissect domain requirement within APE1 for such interaction with NEIL3 Zf-GRF motifs, three mutations in APE1 were produced (E95Q, E95Q-D209N, and D306A). Through GST-pulldown assays, E95Q-D209N, but not E95Q nor D306A mutant APE1 significantly reduced binding to NEIL3-ZF1&2 (Figure 3E). This observation suggests that the D209 residue within APE1 is critical for NEIL3 interaction. We recently revealed that the D209 residue in APE1 active site is important for its endonuclease activity (Lin et al., 2020). Thus, APE1 endonuclease activity may be

regulated by NEIL3 interaction, which warrants further investigation to test this possibility directly.

Because APE1 and APE2 share similar EEP domain, we sought to determine whether NEIL3 Zf-GRF motifs interact with APE2. Our GST-pulldown experiment showed that neither GST-NEIL3-ZF1&2 nor GST-NEIL3-ZF1 associated with Myc-APE2, suggesting no direct interaction between NEIL3 Zf-GRF motifs and APE2 at least under the conditions tested (Figure 3B).

Our lab recently reported that APE2 Zf-GRF associates with PCNA (Lin et al., 2018). Consistent with this, we found that GST-NEIL3-ZF1&2 but not GST associated with His-tagged PCNA *in vitro* (Figure 3C). Notably, GST-NEIL3-ZF1 also interacted with His-tagged PCNA *in vitro* despite a reduction in interaction (almost 50%) compared with the two Zf-GRF motifs (Figure 3C). These observations suggest that one and both NEIL3 Zf-GRF motifs are sufficient for PCNA interaction. Future experiments are needed to determine the critical domains within PCNA and NEIL3 Zf-GRF motifs for this interaction. In addition, prior study has shown that N-terminal domain of NEIL3 is sufficient to interact with PCNA (Zhou et al., 2017). Although the exact underlying mechanism remains unknown, we speculate that NEIL3 may have two different modes of PCNA interaction (one through N-terminal domain, and another one is through Zf-GRF motifs), depending on the context of its complex with DNA and/or other repair proteins.

NEIL3-ZF1&2 binds to shorter ssDNA compared with NEIL3-ZF1

Our recent study has shown that APE2 Zf-GRF motif in APE2 preferentially associated with ssDNA but not dsDNA (Wallace et al., 2017). Although previous study showed that C-terminal domain of NEIL3 was responsible for ssDNA binding (Zhou et al., 2017), the

specific region within the C-terminal domain of NEIL3 for such ssDNA binding has not been identified. Thus, we sought to determine (1) whether NEIL3 Zf-GRF motifs associate with ssDNA; and (2) if so, what aspect of ssDNA binding two Zf-GRF motifs can distinguish from one individual Zf-GRF motif. Through biotin-ssDNA binding assays, GST-NEIL3- ZF1&2 but not GST associated with 60nt, 40nt, 20nt, and as short as 10nt ssDNA (Figure 4A). However, GST-NEIL3- ZF1 but not GST associated with 60nt but not 40nt nor 20nt ssDNA (Figure 4B). These observations suggest that binding to shorter ssDNA via two Zf-GRF motifs may help NEIL3 to function as DNA glycosylase to recognize and remove base damage in short DNA sequences such as replicating forks or telomere regions.

In addition, we failed to express and purify GST-NEIL3-ZF2 recombinant protein after many trials. To test the role of NEIL3 ZF1 for ssDNA binding, we decided to mutate the unique residue in NEIL3-ZF2 from lysine (K) to alanine (A) which is a non-polar amino acid (i.e., GST-NEIL3-ZF1&2-K553A). Amazingly, the binding of GST-NEIL3-ZF1&2-K553A was observed clearly at 20nt and 40nt ssDNA but reduced significantly in 10nt ssDNA (Figure 4C). This observation indicates that the conserved K553 residue within NEIL3-ZF2 is important for binding to short ssDNA (10nt). In conclusion, our findings reveal that two NEIL3 Zf-GRF motifs associate with ssDNA, and that two Zf-GRF motifs but not one individual Zf-GRF motif are needed to bind to shorter ssDNA (10nt). Thus, our findings identified binding to shorter ssDNA as the second feature of Zf-GRF repeat compared with individual Zf-GRF motif.

NEIL3-ZF1&2 interacts with different DNA structures in a sequence-independent manner

Next, we sought to determine the sequence and nature of ssDNA for interacting with NEIL3 Zf-GRF motifs. We utilized EMSA assays with different 5'-FAM labeled ssDNA with or without AP site to quantify the binding ability of NEIL3 Zf-GRF motifs.

Consistent to finding from our biotin DNA-binding assays in Figure 4A, GST-NEIL3-ZF1&2 forms complex with 39nt-ssDNA starting as low as 3 μ M (Figure 5A). Notably, GST-NEIL3-ZF1 did not form a complex with 39nt-ssDNA even under a concentration of 15 μ M (Figure 5B). Furthermore, the complex formation of GST-NEIL3-ZF1&2 - K553A with 39nt-ssDNA was significantly reduced even under the concentration of 15 μ M, suggesting that the K553 residue is important for ssDNA interaction (Figure 5C). We then tested the binding of NEIL3 Zf-GRF motifs to ssDNA which contains an AP site. Interestingly, the presence of an AP site in the 39nt-ssDNA reduced the interactions with GST-NEIL3-ZF1&2, GST-NEIL3-ZF1, and GST-NEIL3-ZF1&2-K553A (Figure 5D-5F). This observation suggests that NEIL3 Zf-GRF motifs do not preferentially associate with AP site on ssDNA.

To determine if the interaction between NEIL3 Zf-GRF motifs and ssDNA is sequence-dependent, we also tested another longer ssDNA (70nt) with different DNA sequence compared with the 39nt-ssDNA. Similar to the binding to 39nt-ssDNA, GST-NEIL3-ZF1&2 associated with 70nt ssDNA at the concentration as low as 3 μ M in EMSA assays (Figure 5G); however, the GST-NEIL3-ZF1&2-K553A mutant showed very weak to almost no binding to 70nt-ssDNA even at the concentration of 15 μ M (Figure 5I).

Notably, GST-NEIL3-ZF1 formed a complex with 70nt-ssDNA at around 15 μ M while such interaction in shorter 39nt-ssDNA was absent (Figure 5B and 5H). This observation is consistent with the finding that GST-NEIL3-ZF1 binds to 60nt-ssDNA but not shorter

ssDNA in our biotin-DNA binding assays (Figure 4B). Interestingly, when biotin was added to the 3' end of 70nt ssDNA, the ZF1&2 motifs and ZF1 motif interaction to ssDNA was remarkably decreased (Figure 5J and 5K). We speculate that the free 3'-end of ssDNA is important for NEIL3 Zf-GRF motifs to start association, or alternatively, that the physical presence of biotin on the 3'-side of ssDNA may compromise the binding of NEIL3 Zf-GRF motifs to ssDNA. More experiments are needed to distinguish from these different scenarios in the future.

NEIL3-ZF1&2 shows higher binding affinity to ssDNA than NEIL3-ZF1

Furthermore, we quantify the binding affinity of NEIL3-ZF1&2, NEIL3-ZF1, and NEIL3-ZF1&2 K553A to ssDNA using MST assays with Cy5-labeled 70nt-ssDNA as substrate (Figure 6A). The substrate was mixed with different concentrations of four ligands for 15 minutes at 25 degree C, respectively (Figure 6A). Notably, we found that GST-NEIL3-ZF1&2 and GST-NEIL3-ZF1, but not GST, associated with Cy5-70nt-ssDNA (Figure 6B). The K_d value for GST-NEIL3-ZF1&2 and GST-NEIL3-ZF1 was $3.9 \pm 0.55 \mu\text{M}$ and $7.9 \pm 0.68 \mu\text{M}$, respectively. The MST observations suggest stronger affinity of two Zf-GRF motifs than one individual Zf-GRF to 70nt-ssDNA. Consistent with our EMSA result (Figure 5I), there were not enough binding points accumulated to generate binding curve for NEIL3-ZF1&2 K553A, suggesting compromised binding of NEIL3-ZF1&2 K553A to 70nt-ssDNA (Figure 6B).

NEIL3-ZF1&2 compromised APE1's endonuclease activity on ssDNA

Our data have revealed that NEIL3-ZF1&2 associate with APE1 and ssDNA (Figures 2-6). To determine the biological significance of the interaction between NEIL3 Zf-GRF motifs and APE1, we aimed to test whether the endonuclease activity of APE1 targeting

AP site on ssDNA or dsDNA is affected by NEIL3 Zf-GRF motifs. Notably, the endonuclease activity of GST-APE1 targeting 5'-FAM-labeled ssDNA with an AP mimicking site was compromised by the addition of GST-NEIL3-ZF1&2 in a dose-dependent manner (Figure 7A). Interestingly, the addition of GST-NEIL3-ZF1 had almost no noticeable effect on the APE1 endonuclease activity targeting AP site on ssDNA (Figure 7B).

To further explore the underlying mechanism of the negative effect on APE1 endonuclease activity targeting AP site on ssDNA by NEIL3-ZF1&2, we tested two different experimental scenarios: shielding effect and inhibition effect. First, for shielding effect experiment, we hypothesize that the negative effect of NEIL3 ZF1&2 is due to its direct interaction to ssDNA-AP to prevent APE1 from recognition and binding to AP site. We incubated NEIL3-ZF1&2 with ssDNA-AP before the addition of GST-APE1 for endonuclease assays and found that once bound with GST-NEIL3-ZF1&2, the 39nt-ssDNA with AP was not cleaved by the GST-APE1 (Figure 7C). This observation supports the shielding effect of NEIL3 Zf-GRF motifs for APE1 endonuclease activity on ssDNA. Second, for inhibition effect experiment, we hypothesize that NEIL3 Zf-GRF motifs may inhibit APE1 endonuclease activity directly since NEIL3-ZF1&2 interacts with APE1 *in vitro*. Thus, we incubated GST-APE1 with GST-NEIL3-ZF1&2 before the addition of ssDNA-AP substrate, and found that the APE1 endonuclease activity targeting AP site on ssDNA was compromised by the preincubation of NEIL3-ZF1&2 too (Figure 7D). This observation suggests that NEIL3 Zf-GRF motifs inhibit APE1 endonuclease activity targeting AP site on ssDNA through direct interaction. This result is also supported by the observation that NEIL3 Zf-GRF motifs interact with APE1

via its active site including the D209 residue shown in Figure 3E. Overall, the shielding effect and inhibition effect are not exclusive to each other.

In addition, we tested the potential effects of NEIL3 Zf-GRF motifs on APE1 endonuclease activity targeting AP site on dsDNA. We found that increasing doses of NEIL3-ZF1&2 had almost no effect on the cleavage of 5'-FAM-dsDNA39-AP by GST-APE1 (Figure 7E). Furthermore, as APE1 displays faster or very robust AP endonuclease activity targeting AP site on dsDNA, we sought to determine whether APE1 endonuclease activity on dsDNA at low doses is affected by NEIL3 Zf-GRF motifs. We tested APE1 endonuclease assays on dsDNA with series dilutions of APE1 and found that the addition of NEIL3-ZF1&2 had almost no effects on APE1 endonuclease activity on dsDNA (Figure 7F). Although NEIL3 Zf-GRF motifs interact with APE1, we confirm that APE1 endonuclease activity on dsDNA is not affected by NEIL3 Zf-GRF motifs.

NEIL3-ZF1&2 motifs form dimerization or higher order oligomerization

One distinct feature observed in EMSA results was the presence of two major bands when NEIL3-ZF1&2 interacted with ssDNA while only one band was detected when NEIL3-ZF1 motif interacted with ssDNA (Figure 5). We reasoned that the two NEIL3 Zf-GRF motifs may form dimerization or oligomerization. To test this possibility directly, we performed GST-pulldown assays and found that GST-NEIL3-ZF1&2 but not GST can pulldown Myc-NEIL3-ZF1&2, suggesting dimerization or oligomerization of NEIL3 Zf-GRF motifs (Figure 8A). We also noticed that the binding of Myc-NEIL3-ZF1 and Myc-NEIL3-ZF2 to GST-NEIL3-ZF1&2 was decreased (~50% - 70%) in comparison to Myc-NEIL3-ZF1&2 (Figure 8A). Furthermore, GST-NEIL3-ZF1 can pulldown Myc-NEIL3-ZF1&2 but neither Myc-NEIL3-ZF1 nor Myc-NEIL3-ZF2,

suggesting that NEIL3 ZF1 can't form homodimer with another ZF1 nor heterodimer with ZF2 (Figure 8B). These observations strongly support that NEIL3 Zf-GRF repeat forms dimerization or oligomerization, which requires both Zf-GRF motifs but not one individual Zf-GRF motif.

If NEIL3 Zf-GRF repeat forms homodimer, we would be able to observe this on a native PAGE gel. When purified GST-NEIL3-ZF1&2 was resolved on native-PAGE, two visible bands were observed, suggesting that two NEIL3 Zf-GRF motifs form complexes prior to DNA/protein interaction (Figure 8C). We also noted that the K553A mutant in GST-NEIL3-ZF1&2 had almost no effect on the formation of complexes (Figure 8D). Interestingly, there is almost only one band was observed when recombinant GST-NEIL3-ZF1 protein was resolved on native PAGE (Figure 8E).

Thus, we confirmed that NEIL3 Zf-GRF repeat exists as complexes (dimer or oligomer) even before the presence of DNA/proteins. Although we do not know if ssDNA interaction and Zf-GRF repeat dimerization affect each other, we did observe that there were two bands of ssDNA-NEIL3-ZF1&2 complexes (Figure 5). Further structural analysis is needed to figure out the exact underlying mechanism.

CHAPTER 3: DISCUSSION AND FUTURE DIRECTIONS

APE1 cleaves AP site on both ssDNA and dsDNA although the AP endonuclease was rather weak on ssDNA. Nevertheless, APE1 definitely could generate SSBs from ssDNA. Thus, it is extremely important for cells to prevent SSB formation in ssDNA regions in the genome. Therefore, it is significant to determine how APE1 endonuclease activity targeting AP site on ssDNA is regulated, especially in the consideration of both APE1 and NEIL3 are functional at telomeres (Zhou et al., 2017). Our findings suggest a potential function of NEIL3-GRF-ZF1&2 in the regulation of APE1's endonuclease activity. In my MS thesis, I have demonstrated (1) that NEIL3 Zf-GRF motifs interact with APE1 and PCNA, but not APE2 (Figure 2-3); (2) NEIL3 ZF1&2 associated with shorter ssDNA than one Zf-GRF motif (Figure 4); (3) NEIL3 ZF1&2 displays higher affinity to ssDNA than one Zf-GRF motif (Figure 5-6); (4) NEIL3 ZF1&2 formed complexes with itself; and (5) APE1's endonuclease on ssDNA but not dsDNA was compromised with the presence of NEIL3 ZF1&2. Based on these findings, we have identified a previously uncharacterized negative regulation of APE1 endonuclease on ssDNA by NEIL3 Zf-GRF motifs.

We propose a working model to show the significance of APE1 regulation by NEIL3 in BER pathway (Figure 9). Base damage is recognized and removed by NEIL3 to generate an AP site on ssDNA region at replication fork or at telomeres. With the presence of NEIL3 ZF1&2, the AP site on ssDNA may be shield from APE1's endonuclease activity by two Zf-GRF motifs binding to ssDNA, or NEIL3 Zf-GRF repeat may interact with APE1 directly and compromise its endonuclease activity. Without NEIL3-ZF1&ZF2, the AP site on ssDNA is recognized and cleaved by APE1 to generate SSBs, which represent

a threat to genome stability. This mechanism also explains why NEIL3 is highly expressed in S and G2/S phase when long ssDNA is generated.

Thus, our results support the negative regulation of APE1 endonuclease activity on ssDNA but not on dsDNA by NEIL3 Zf-GRF motifs. Our results have demonstrated two potential mechanisms of NEIL3-ZF1&2 function as (1) NEIL3 Zf-GRF motifs shield ssDNA-AP from APE1 endonuclease function and (2) NEIL3 Zf-GRF motifs interact and inhibit APE1 endonuclease function. These two effects were very unique and critical for ssDNA stability considering APE1 could generate SSBs, leading to genetic instability. Our findings not only identified the new interaction between APE1 and NEIL3 Zf-GRF motifs but also revealed that APE1 endonuclease activity on ssDNA is negatively regulated by NEIL3 Zf-GRF motifs. Our findings are of significance because ssDNA exists in replication fork and telomeres where a single base damage could trigger BER in cells. Taken together, our findings suggest a critical regulation of APE1 function in genome integrity by NEIL3.

In the future, we may need to work on a couple of directions: (1) express and purify recombinant NEIL3-ZF2 to directly compare its features with NEIL3-ZF1; (2) structural analysis of the interaction between NEIL3 ZF1&2 and APE1 with or without the presence of ssDNA with or without AP site; (3) analysis of the interaction between ssDNA containing telomere specific sequence and NEIL3 Zf-GRF motifs. In addition, it will be very interesting to test whether Zf-GRF repeat-containing protein Top3 alpha also interacts with APE1 and ssDNA.

NEIL3 has been implicated in the BER and inter-strand crosslink repair (Semlow et al., 2016; Zhou et al., 2017), while APE1 has been shown to be critical for DNA repair,

transcriptional regulation, and DDR pathways (Dyrkheeva et al., 2016; Lin et al., 2020). Our findings shed new light on the regulation of APE1 endonuclease activity on ssDNA by NEIL3 Zf-GRF motifs. Our research may provide novel avenue to therapeutic treatment for cancer patients with abnormal expression or mutants of APE1 and NEIL3.

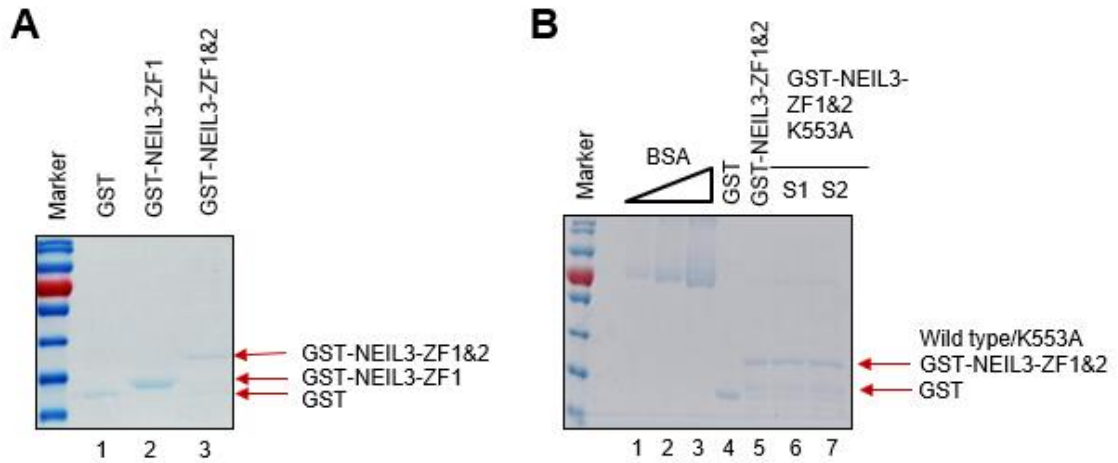


Figure 2: Coomassie protein expression verification for GST-NEIL3-ZF1 and GST-NEIL3-ZF1&2 and GST-NEIL3-ZF1&2 K553A. (A) GST-NEIL3-ZF1&2 and GST-NEIL3-ZF1 expression detected with GST as control on PAGE. (B) GST-NEIL3-ZF1&2 K553A expression using GST as negative control while BSA different doses as base line for comparison concentration of ZF1&2 K553A detected.

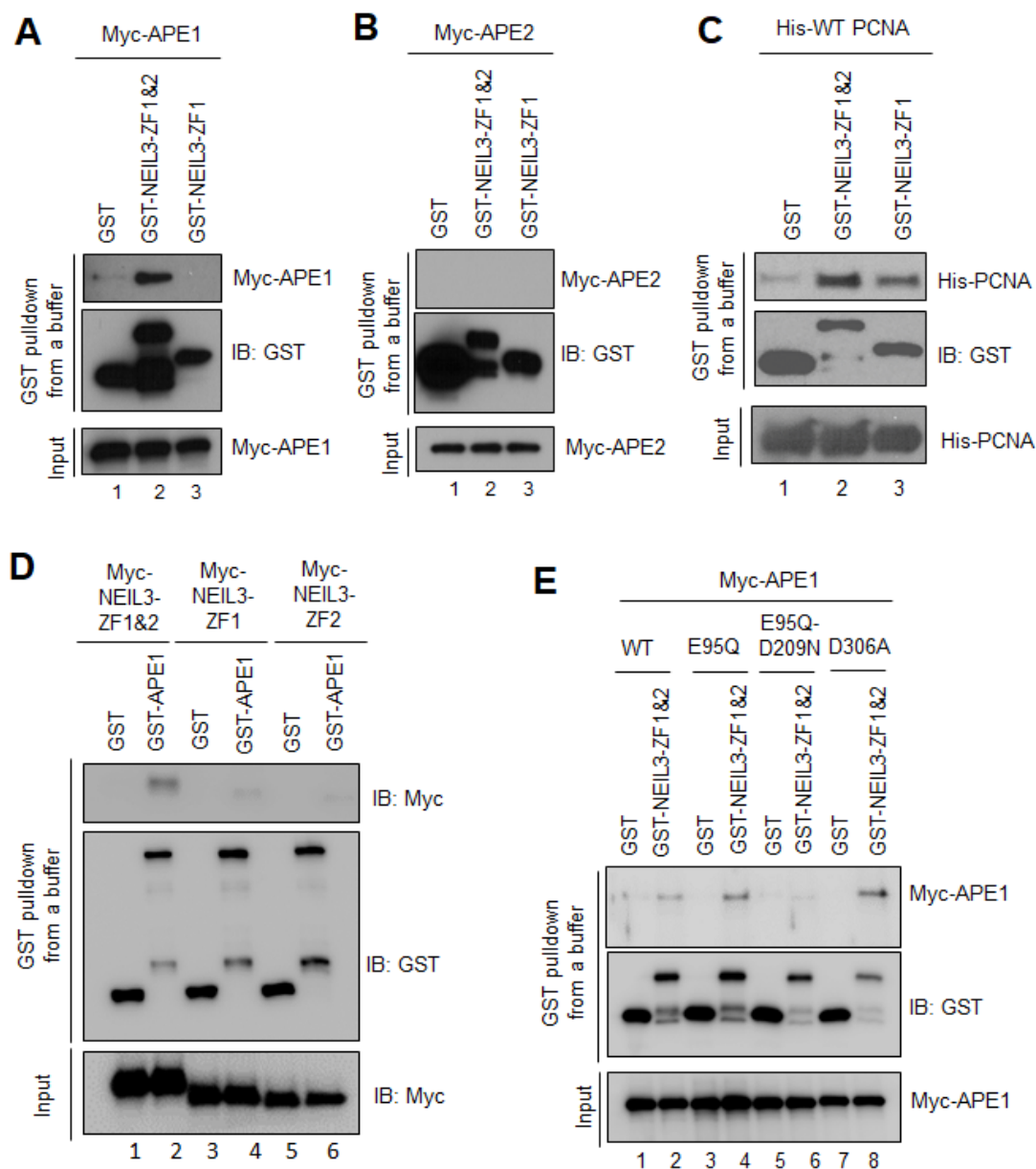


Figure 3: NEIL3-ZF1&2 interacts with APE1 and PCNA but not APE2 *in vitro*. (A) GST-pull-down assay performed between Myc-APE1 and GST-NEIL3-ZF1&2, GST-NEIL3-ZF1, or GST *in vitro*. (B) Interaction between Myc-APE2 and GST-NEIL3-ZF1&2, GST-NEIL3-ZF1, or GST. (C) Interaction of GST-NEIL3-ZF1&2 to His-PCNA was detected while GST-NEIL3-ZF1 had almost 50% reduction in interaction to His-PCNA. (D) GST-pull-down assay expanded to detect interaction between Myc-NEIL3-ZF1&2/ Myc-NEIL3-ZF1/ Myc-NEIL3-ZF2 and GST-APE1 *in vitro*. (E) Myc-APE1 WT, E95Q, E95Q-D209N, or D306A interaction with GST-NEIL3-ZF1&2 for determining the possible region within APE1 for such interaction.

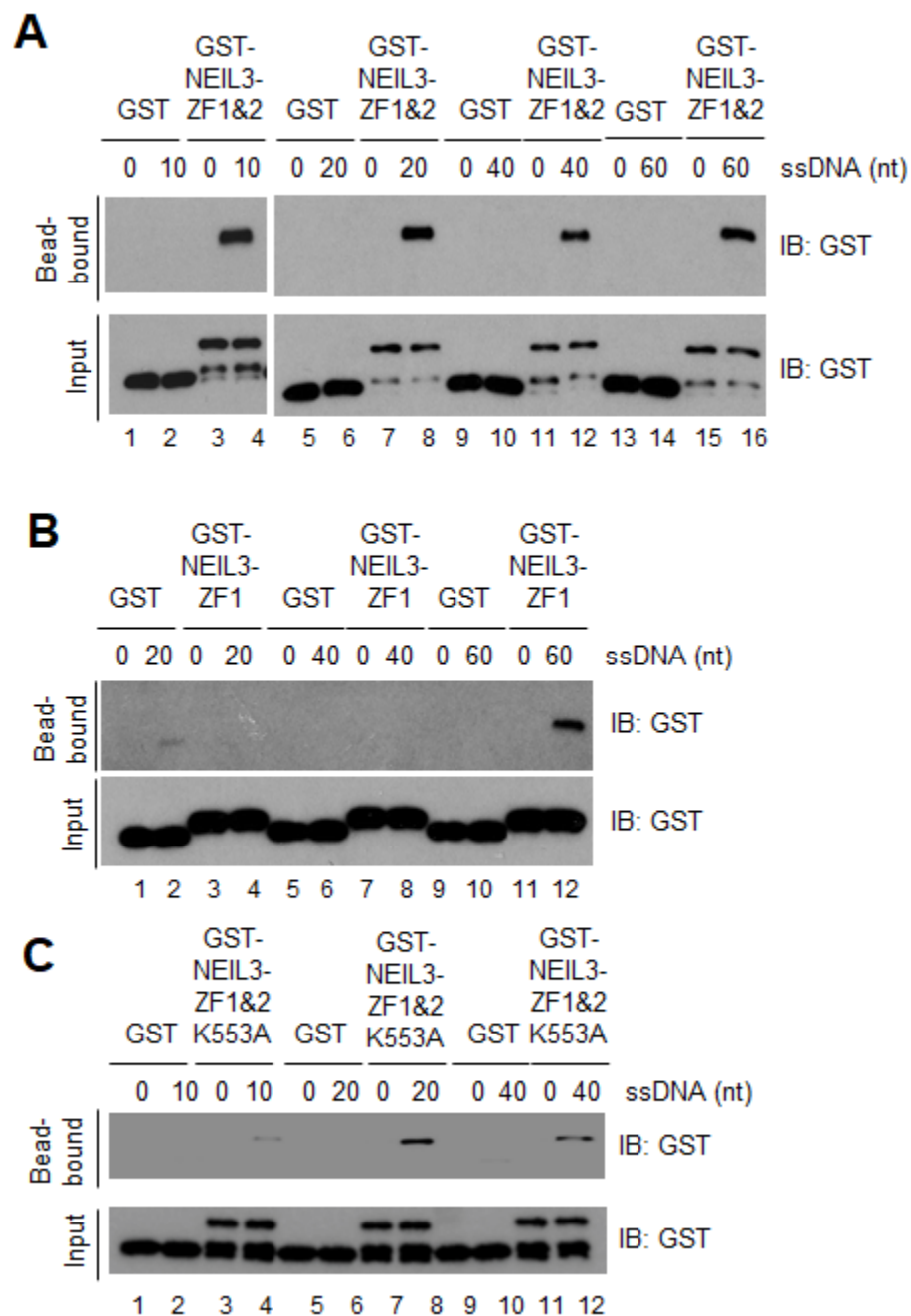


Figure 4: NEIL3-ZF1&2 binds to shorter ssDNA than NEIL3-ZF1. (A) Interaction between GST-NEIL3-ZF1&2 and biotin-labeled ssDNA structure of 10, 20, 40, 60nt via biotin-DNA binding assays. (B) The interaction of GST-NEIL3-ZF1 and different biotin labeled ssDNA structure of 20, 40, 60nt. (C) Interaction of GST-NEIL3-ZF1&2 K553A and biotin-ssDNA structure of 10, 20, 40nt via biotin-DNA binding assays.

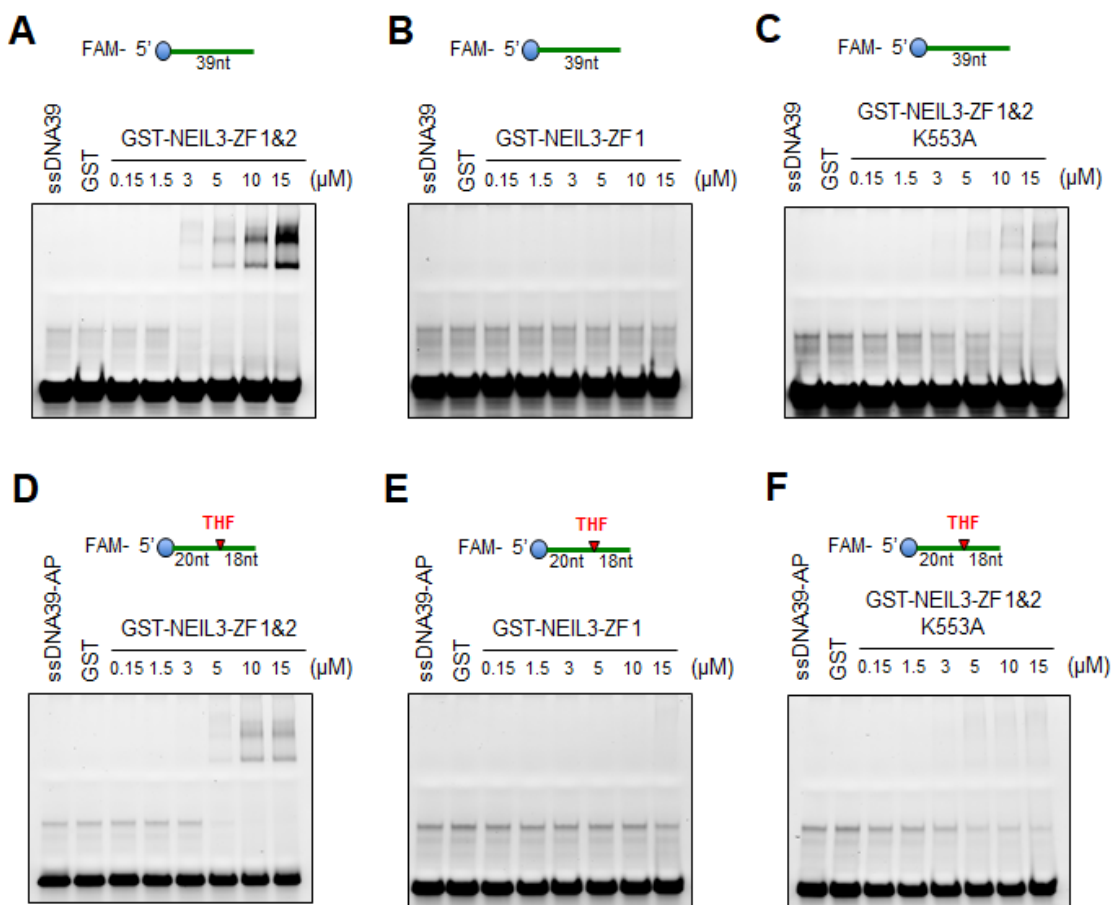


Figure 5: NEIL3-ZF1&2 interacts with different ssDNA structures. (A-C) EMSA assays show the interaction detected between 5'-FAM-ssDNA39 GST-NEIL3-ZF1&2, GST-NEIL3-ZF1, or GST-NEIL3-ZF1&2 K553A at different doses indicated in 60 minutes/room temperature. (D-F) EMSA assays reveal interaction between 5'-FAM-ssDNA39-AP and increased concentrations of GST-NEIL3-ZF1&2 or GST-NEIL3-ZF1 or GST-NEIL3-ZF1&2 K553A *in vitro*.

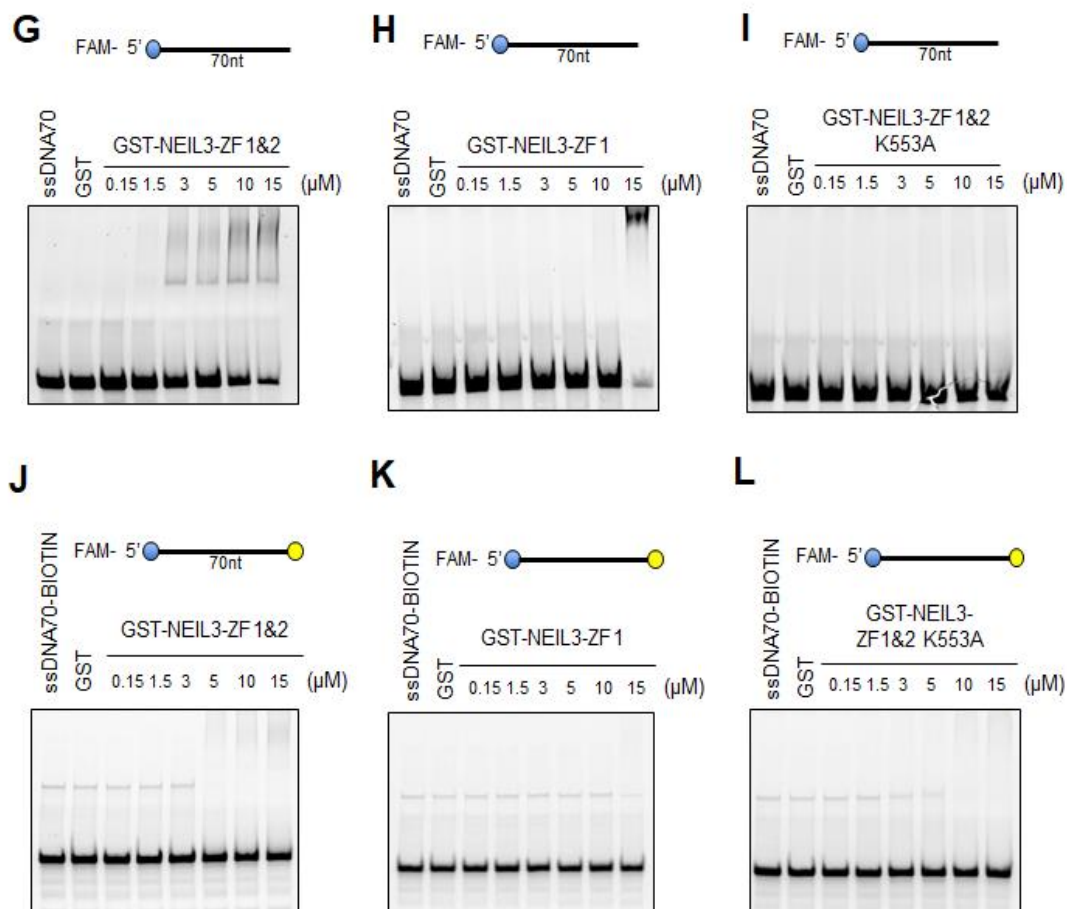


Figure 5: NEIL3-ZF1&2 interacts with different ssDNA structures-continued. (G-I) Interaction between 5'-FAM-ssDNA70 and GST-NEIL3-ZF1&2 or GST-NEIL3-ZF1 detected but not with GST-NEIL3-ZF1&2 K553A via EMSA assays. 5'-FAM-ssDNA70 sequence generated was completely different from 5'-FAM-ssDNA39 and 5'-FAM-ssDNA39-AP. (J-L) EMSA assays show interaction between 5'-FAM-ssDNA70-Biotin-3' and GST-NEIL3-ZF1&2, GST-NEIL3-ZF1 or GST-NEIL3-ZF1&2 K553A.

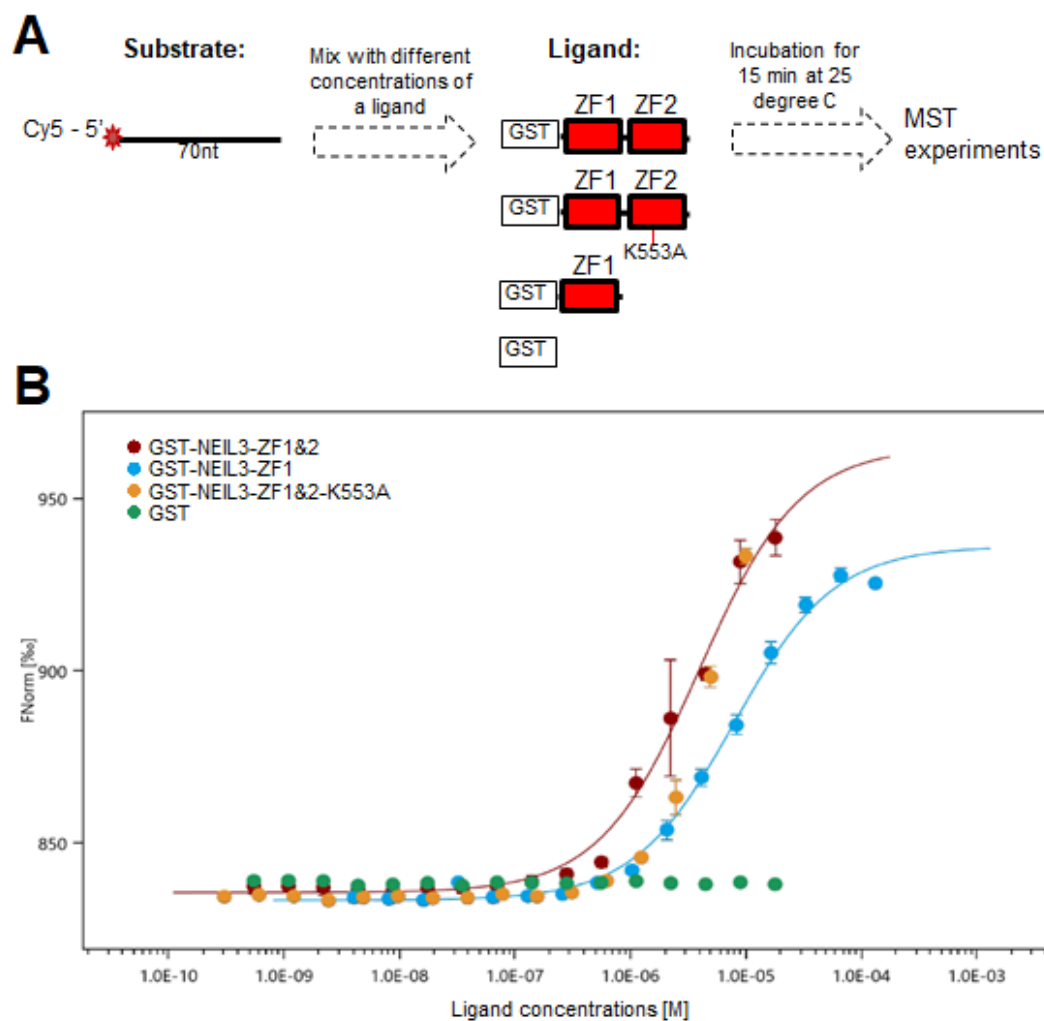


Figure 6: MST assays show NEIL3-ZF1&2 motifs have higher binding affinity to Cy5-labelled 70-nt ssDNA than NEIL3-ZF1. (A) Diagram showed the overall steps and condition used for MST experiments including the structure of substrate (target) and structure of each of four ligands. (B) Binding curves constructed for NEIL3-ZF1&2 (n=4), NEIL3-ZF1 (n=3), and NEIL3-ZF1&2 K553A (n=3) with GST (n=3) as control using 50nM of Cy5-labelled ssDNA in Buffer A. F_{norm} is normalized fluorescence which is measured by F_1 as fluorescence after thermodiffusion (at 4-5seconds range) divided by F_0 as initial fluorescence.

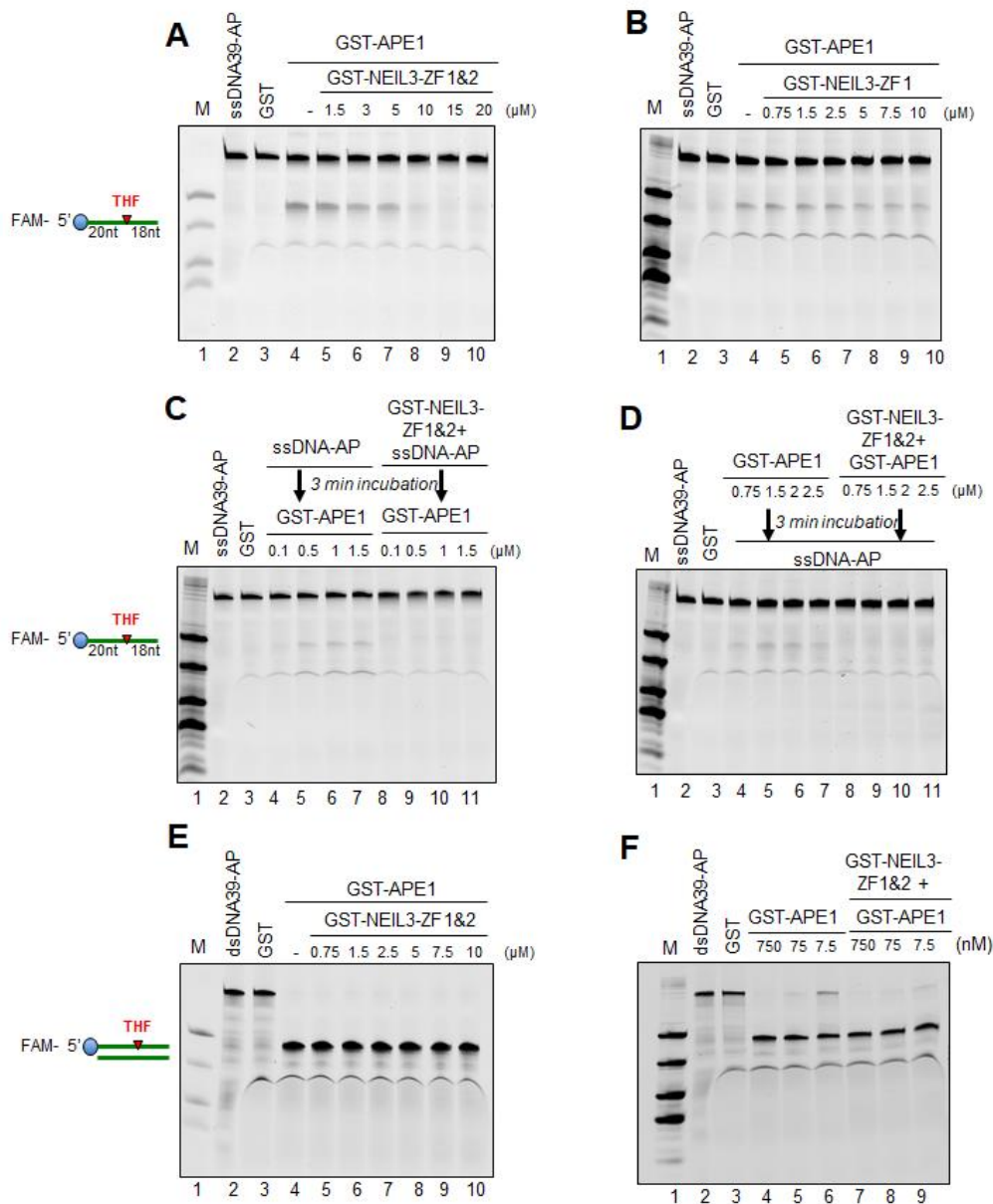


Figure 7: NEIL3-ZF1&2 compromises APE1's endonuclease activity on ssDNA. (A) Endonuclease assay using 5'-FAM-ssDNA39-AP in the presence of GST-APE1 with or without GST-NEIL3-ZF1&2 at different doses. (B) Similar assay repeated using different doses of GST-NEIL3-ZF1 instead for detecting any effects on APE1's endo activity. (C) 5'-FAM-ssDNA39-AP with or without GST-NEIL3-ZF1&2 incubated at 37°C for 3 min before the addition of GST-APE1 at various doses indicated then incubated at 37°C for 60 min for shielding effect of NEIL3-ZF1&2 on ssDNA-AP. (D) Different doses of GST-APE1 incubated with or without GST-NEIL3-ZF1&2 at 37°C for 3 min before the addition of FAM-ssDNA39-AP for another 60 min-incubation for inhibition effect through direct interaction between two proteins. (E) GST-APE1 endonuclease activity detected with or without the presence of different doses of GST-NEIL3-ZF1&2 using FAM-dsDNA39-AP as substrate. (F) Effect of GST-NEIL3-ZF1&2 on GST-APE1 endo activity targeting FAM-dsDNA39-AP using different concentration of GST-APE1.

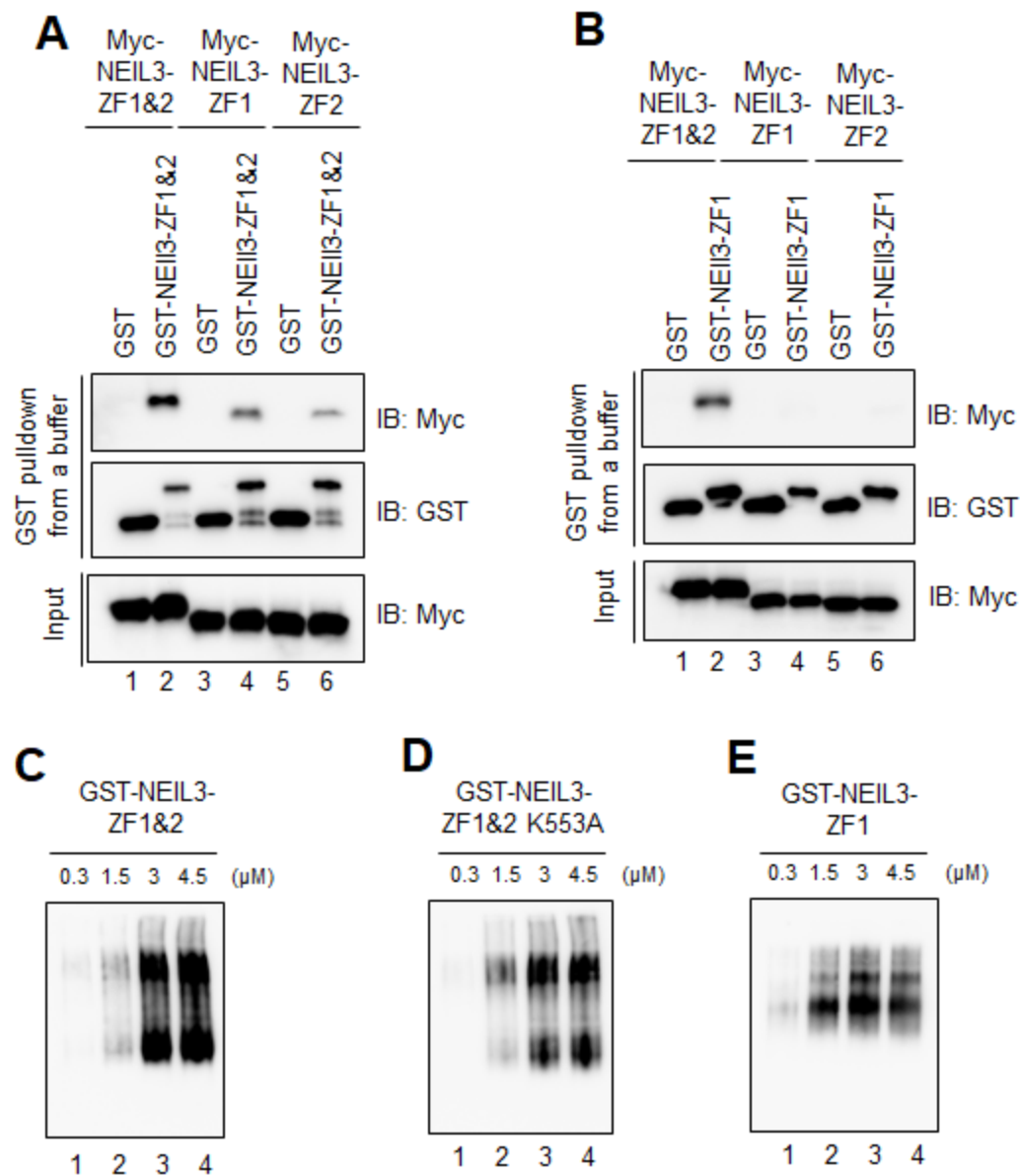


Figure 8: NEIL3-ZF1&2 forms complexes with itself. (A) Interaction detected between GST-NEIL3-ZF1&2 and Myc-NEIL3-ZF1&2 while significant reduction was detected when GST-NEIL3-ZF1&2 interacted to Myc-NEIL3-ZF1 and Myc-NEIL3-ZF2. (B) Interaction detected between GST-NEIL3-ZF1 and Myc-NEIL3-ZF1&2 but not Myc-NEIL3-ZF1 or Myc-NEIL3-ZF2. (C-E) Native gel electrophoresis performed on GST-NEIL3-ZF1&2, GST-NEIL3-ZF1, and GST-NEIL3-ZF1&2 K553A at different concentrations as indicated.

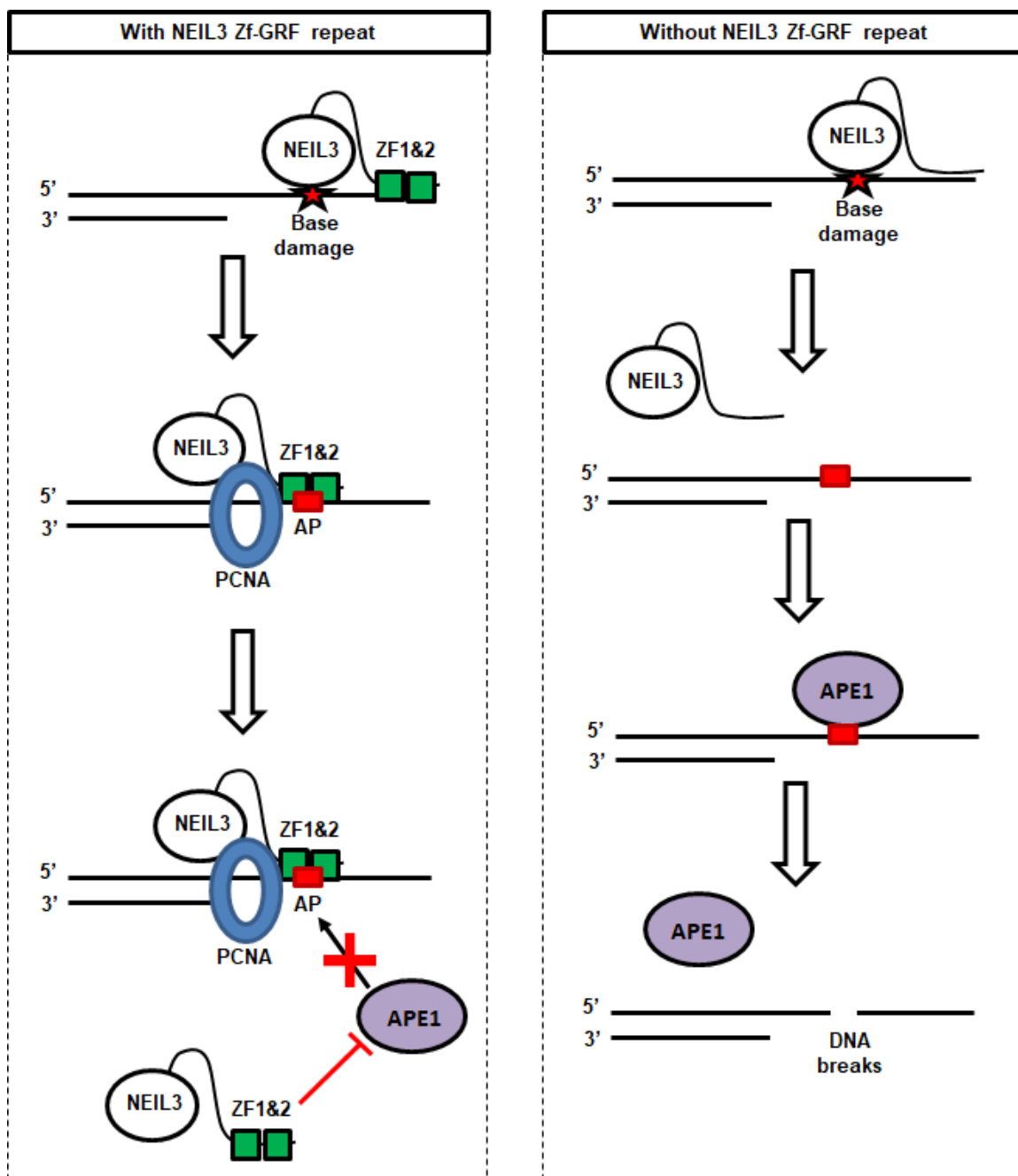


Figure 9: A working model of the regulation of APE1's endonuclease activity on ssDNA by NEIL3-ZF1&2. Base damage is recognized and removed by NEIL3. With the presence of NEIL3 Zf-GRF motifs, AP site may be shielded from APE1's endo activity (shielding effect). Alternatively, NEIL3 Zf-GRF motifs may interact with APE1 and inhibit its AP endonuclease activity (inhibition effect). With the absence of NEIL3 Zf-GRF motifs, APE1 recognizes the AP site and cleaves it into DNA break, leading to genome instability. This mechanism of NEIL3 ZF1&2 prevented ssDNA breakage and DNA shortening by APE1's operation. The figure used monomer NEIL3-ZF1&2 with several proteins deleted for basic illustration.

REFERENCES

- Burkovics, P., Hajdu, I., Szukacsov, V., Unk, I., & Haracska, L. (2009, Jul). Role of PCNA-dependent stimulation of 3'-phosphodiesterase and 3'-5' exonuclease activities of human Ape2 in repair of oxidative DNA damage. *Nucleic Acids Res.*, 37(13), 4247-4255. <https://doi.org/10.1093/nar/gkp357>
- Cassandri, M., Smirnov, A., Novelli, F., Pitolli, C., Agostini, M., Malewicz, M., Melino, G., & Raschella, G. (2017). Zinc-finger proteins in health and disease. *Cell Death Discov*, 3, 17071. <https://doi.org/10.1038/cddiscovery.2017.71>
- Ciccia, A., & Elledge, S. J. (2010, Oct 22). The DNA damage response: making it safe to play with knives. *Mol Cell*, 40(2), 179-204. <https://doi.org/10.1016/j.molcel.2010.09.019>
- Cupello, S., Richardson, C., & Yan, S. (2016). Cell-free *Xenopus* egg extracts for studying DNA damage response pathways. *Int J Dev Biol*. 60 (7-8-9): 229-236. <http://dx.doi.org/10.1387/ijdb.160113sy>
- Cupello, S., Lin, Y., & Yan, S. (2019). Distinct roles of XRCC1 in genome integrity in *Xenopus* egg extracts. *Biochem J*. 476(24):3791-3804. <https://doi.org/10.1042/BCJ20190798>
- Dyrkheeva, N. S., Lebedeva, N. A., & Lavrik, O. I. (2016, Sep). AP Endonuclease 1 as a key enzyme in repair of apurinic/apyrimidinic sites. *Biochemistry (Mosc)*, 81(9), 951-967. <https://doi.org/10.1134/S0006297916090042>
- Jacobs, A. L., & Schar, P. (2012, Feb). DNA glycosylases: in DNA repair and beyond. *Chromosoma*, 121(1), 1-20. <https://doi.org/10.1007/s00412-011-0347-4>

- Jensen, K. A., Shi, X., & Yan, S. (2020). Genomic alterations and abnormal expression of APE2 in multiple cancers. *Sci Rep*, *10*(1). <https://doi.org/10.1038/s41598-020-60656-5>
- Krokan, H. E., & Bjoras, M. (2013, Apr 1). Base excision repair. *Cold Spring Harb Perspect Biol*, *5*(4), a012583. <https://doi.org/10.1101/cshperspect.a012583>
- Lin, Y., Bai, L., Cupello, S., Hossain, M. A., Deem, B., McLeod, M., Raj, J., & Yan, S. (2018, Mar 16). APE2 promotes DNA damage response pathway from a single-strand break. *Nucleic Acids Res.*, *46*(5), 2479-2494. <https://doi.org/10.1093/nar/gky020>
- Lin, Y., Ha, Anh., & Yan, S. (2019). Methods for studying DNA single-strand break repair and signaling in *Xenopus* egg extracts. *Methods Mol Biol.* 1999: 161-172. https://doi.org/10.1007/978-1-4939-9500-4_9
- Lin, Y., Raj, J., Li, J., Ha, A., Hossain, M. A., Richardson, C., Mukherjee, P., & Yan, S. (2020, Feb 28). APE1 senses DNA single-strand breaks for repair and signaling. *Nucleic Acids Res.*, *48*(4), 1925-1940. <https://doi.org/10.1093/nar/gkz1175>
- Manoel-Caetano, F. S., Rossi, A. F. T., Calvet de Moraes, G., Severino, F. E., & Silva, A. E. (2019, Jun). Upregulation of the APE1 and H2AX genes and miRNAs involved in DNA damage response and repair in gastric cancer. *Genes Dis*, *6*(2), 176-184. <https://doi.org/10.1016/j.gendis.2019.03.007>
- Prakash, A., & Doublet, S. (2015, Aug). Base Excision Repair in the Mitochondria. *J Cell Biochem*, *116*(8), 1490-1499. <https://doi.org/10.1002/jcb.25103>

- Prakash, A., Doublet, S., & Wallace, S. S. (2012). The Fpg/Nei family of DNA glycosylases: substrates, structures, and search for damage. *Prog Mol Biol Transl Sci*, 110, 71-91. <https://doi.org/10.1016/B978-0-12-387665-2.00004-3>
- Qing, Y., Li, Q., Ren, T., Xia, W., Peng, Y., Liu, G. L., Luo, H., Yang, Y. X., Dai, X. Y., Zhou, S. F., & Wang, D. (2015). Upregulation of PD-L1 and APE1 is associated with tumorigenesis and poor prognosis of gastric cancer. *Drug Des Devel Ther*, 9, 901-909. <https://doi.org/10.2147/DDDT.S75152>
- Ray, P. D., Huang, B. W., & Tsuji, Y. (2012, May). Reactive oxygen species (ROS) homeostasis and redox regulation in cellular signaling. *Cell Signal*, 24(5), 981-990. <https://doi.org/10.1016/j.cellsig.2012.01.008>
- Semlow, D. R., Zhang, J., Budzowska, M., Drohat, A. C., & Walter, J. C. (2016, Oct 6). Replication-Dependent Unhooking of DNA Interstrand Cross-Links by the NEIL3 Glycosylase. *Cell*, 167(2), 498-511 e414. <https://doi.org/10.1016/j.cell.2016.09.008>
- Shinmura, K., Kato, H., Kawanishi, Y., Igarashi, H., Goto, M., Tao, H., Inoue, Y., Nakamura, S., Misawa, K., Mineta, H., & Sugimura, H. (2016). Abnormal Expressions of DNA Glycosylase Genes NEIL1, NEIL2, and NEIL3 Are Associated with Somatic Mutation Loads in Human Cancer. *Oxid Med Cell Longev*, 2016, 1546392. <https://doi.org/10.1155/2016/1546392>
- Sokalingam, S., Raghunathan, G., Soundrarajan, N., & Lee, S. G. (2012). A study on the effect of surface lysine to arginine mutagenesis on protein stability and structure using green fluorescent protein. *PloS One*, 7(7), e40410. <https://doi.org/10.1371/journal.pone.0040410>

- Wallace, B. D., Berman, Z., Mueller, G. A., Lin, Y., Chang, T., Andres, S. N., Wojtaszek, J. L., DeRose, E. F., Appel, C. D., London, R. E., Yan, S., & Williams, R. S. (2017, Jan 10). APE2 Zf-GRF facilitates 3'-5' resection of DNA damage following oxidative stress. *Proc Natl Acad Sci U S A*, *114*(2), 304-309. <https://doi.org/10.1073/pnas.1610011114>
- Willis, J., Patel, Y., Lentz, B. L., & Yan, S. (2013, Jun 25). APE2 is required for ATR-Chk1 checkpoint activation in response to oxidative stress. *Proceedings of the National Academy of Sciences of the United States of America*, *110*(26), 10592-10597. <https://doi.org/10.1073/pnas.1301445110>
- Wu, R. A., Semlow, D. R., Kamimae-Lanning, A. N., Kochenova, O. V., Chistol, G., Hodskinson, M. R., Amunugama, R., Sparks, J. L., Wang, M., Deng, L., Mimoso, C. A., Low, E., Patel, K. J., & Walter, J. C. (2019, Mar). TRAIIP is a master regulator of DNA interstrand crosslink repair. *Nature*, *567*(7747), 267-272. <https://doi.org/10.1038/s41586-019-1002-0>
- Xanthoudakis, S., Smeyne, R. J., Wallace, J. D., & Curran, T. (1996, Aug 20). The redox/DNA repair protein, Ref-1, is essential for early embryonic development in mice. *Proceedings of the National Academy of Sciences of the United States of America*, *93*(17), 8919-8923. <https://doi.org/10.1073/pnas.93.17.8919>
- Yan, S., Willis, J. (2013). WD40-repeat protein WDR18 collaborates with TopBP1 to facilitate DNA damage checkpoint signaling. *Biochem Biophys Res Commun.* *431* (2): 466-471. <http://dx.doi.org/10.1016/j.bbrc.2012.12.144>

Yan, S., Sorrell, M., & Berman, Z. (2014, Oct). Functional interplay between ATM/ATR-mediated DNA damage response and DNA repair pathways in oxidative stress.

Cell Mol Life Sci, 71(20), 3951-3967. <https://doi.org/10.1007/s00018-014-1666-4>

Zhou, J., Chan, J., Lambele, M., Yusufzai, T., Stumpff, J., Opresko, P. L., Thali, M., & Wallace, S. S. (2017, Aug 29). NEIL3 Repairs Telomere Damage during S Phase to Secure Chromosome Segregation at Mitosis. *Cell Rep*, 20(9), 2044-2056.

<https://doi.org/10.1016/j.celrep.2017.08.020>